

Conductivity Behaviour of Thick-film Tin Dioxide Gas Sensors

F.-J. SCHMITTE

Uni-GH-Paderborn FB16 Elektrische Energietechnik, Steingraben 21, D-4770 Soest (F.R.G.)

G. WIEGLEB*

Leopold Kostal GmbH and Co. KG, Wiesenstrasse 47, D-5880 Lüdenscheid (F.R.G.)

Abstract

SnO_2 semiconductor gas sensors undoped and doped with Pt and Pd are prepared by the thick-film technique on Al_2O_3 substrates with different electrode structures. The SnO_2 layer structure is characterized by scanning electron microscopy (SEM) and X-ray diffraction. The temperature dependence of the conductance of these sensors is measured by d.c. and a.c. techniques up to 300 kHz in the temperature range 300 to 800 K under synthetic air and air/250 ppm CO mixtures, as well as the sensor response time due to gas changes from air to air/CO.

The results show a temperature-activated conduction mechanism which is discussed using a barrier model. The response time is governed by diffusion processes of the gas into the porous SnO_2 layer and surface reaction times.

Introduction

Gas sensors based on tin dioxide have a variety of applications in monitoring flammable and toxic gases [1]. In automotive applications these sensors are used to keep track of the CO concentration in the car interior and to control the flow of fresh air [2, 3]. Such sensors should have a short response time, and their production cost should be as low as possible. Sensors manufactured

by the thick-film technique fulfil these requirements [4]. Sensors made from a thick-film paste of SnO_2 powder should have the same conductivity behaviour as commercial gas sensors (e.g., TGS 812). The scope of this work is the investigation of the structure and temperature dependence of the conductance of thick-film SnO_2 sensors and their sensitivity and response time.

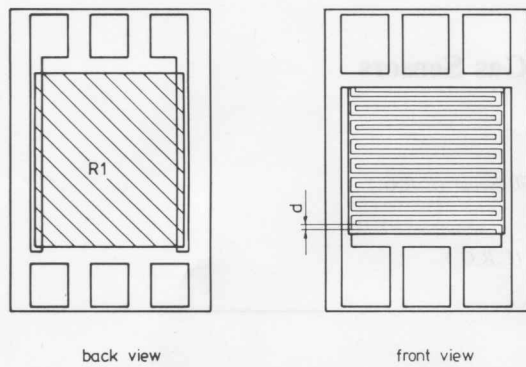
Experimental

The thick-film sensors consisted of gold conduction electrodes covered by a SnO_2 layer on one side of the Al_2O_3 substrate. Sensors with gold electrode spacings of 40, 200 and 400 μm were prepared by usual thick-film techniques. A heater consisting of a commercial resistor paste ($R_{\square} = 7 \Omega$) was printed on the other side of the substrate (Fig. 1). Typical dimensions of the sensor and the heater layer were 8 mm \times 8 mm and the layer thickness in all cases was 15 μm . This gives a heating power of approximately 0.1 W/ mm^2 at 450 $^{\circ}\text{C}$. The SnO_2 paste had a composition of 71% SnO_2 powder (Merck no. 7818), 5% glass powder with solvents and adhesives. All layers were fired by a 850 $^{\circ}\text{C}$ temperature profile for 1 h.

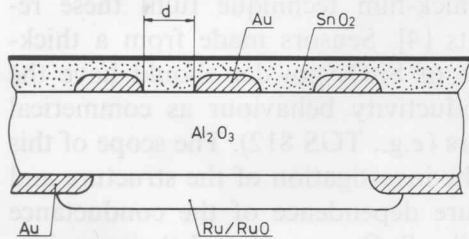
Some sensors were provided with Pt or Pd catalysts by applying ammonium hexachloroplatinate or -paladate to the sensor surface and firing again at 600 $^{\circ}\text{C}$ and 850 $^{\circ}\text{C}$, respectively.

X-ray diffraction measurements were performed with a separately printed SnO_2 layer

*Present address: Hartmann and Braun AG, Heerstrasse 6, Frankfurt/Main, F.R.G.



(a)

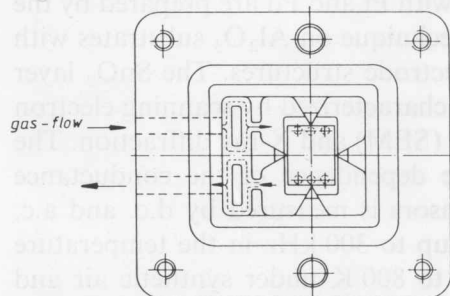
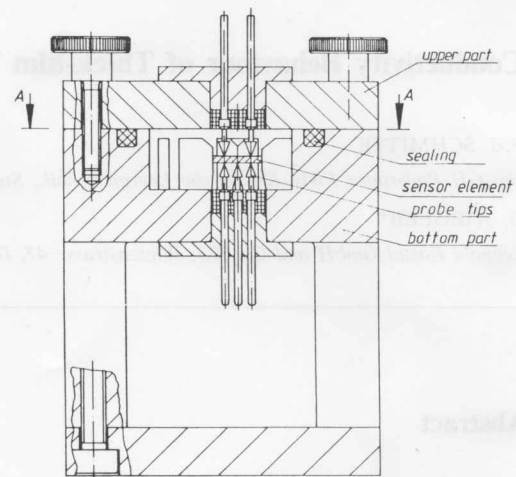


(b)

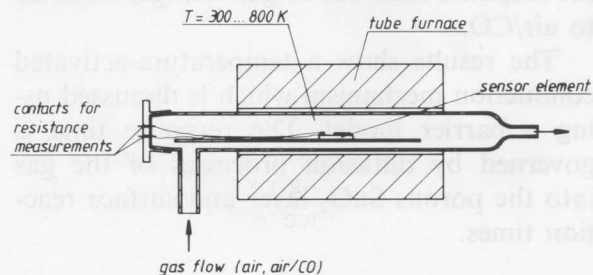
Fig. 1. Plane electrode design of the heater (back side) and gas-sensitive layer (front side) (a) and cross section of the thick-film structure (b).

as well as SEM pictures to determine the structure of the layer. The measurement of the temperature dependence of the resistance in the range 300 to 800 K was done in two different test chambers (Fig. 2). In the first test chamber the electrical contacts to the sensor element were made by probe needles and the sensor temperature was controlled by the heater current. Resistance monitoring of the SnO_2 layer was done with a Keithley 197 microvoltmeter and a test gas mixture of synthetic air (80% N_2 , 20% O_2) or synthetic air + 250 ppm CO with a flow rate of 0.5 l/min was allowed to flow through the chamber.

In the second test chamber the sensor and the gas were heated by a tube furnace. The electrical contacts must therefore maintain temperatures up to 500 °C and consisted of Ag/Pd wire which was soldered with Ag thick-film paste to the gold contact pads [5]. The gas flow rate in this case was 0.002 l/h. Due to the high resistance of the sensor elements at room temperature of about 110 M Ω , the resistance was calculated from



(a)



(b)

Fig. 2. Cross sections of the test chambers I(a) and II(b).

the current measured with a lock-in amplifier after applying a constant a.c. voltage of 0.1 V and 118 Hz. The frequency dependence of the sensor impedance was determined by using a precision LCR meter (HP 4284A).

Experimental Results and Discussion

SEM pictures show that the SnO_2 thick-film layers are very porous with grain

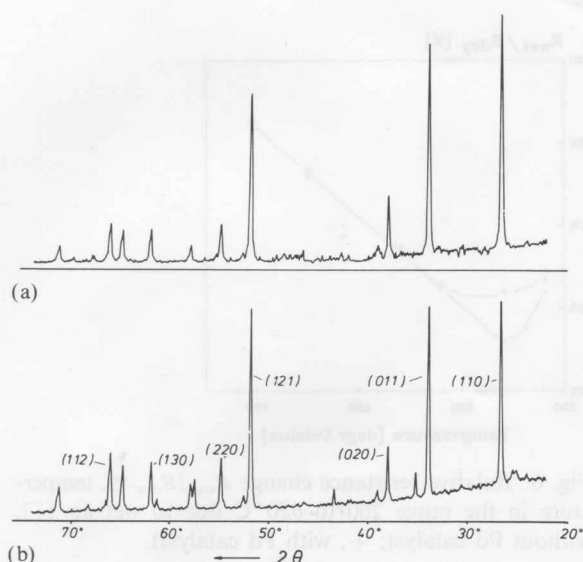


Fig. 3. Diffraction diagram of SnO_2 powder (a) and SnO_2 thick-film layer on an alumina substrate after firing (b).

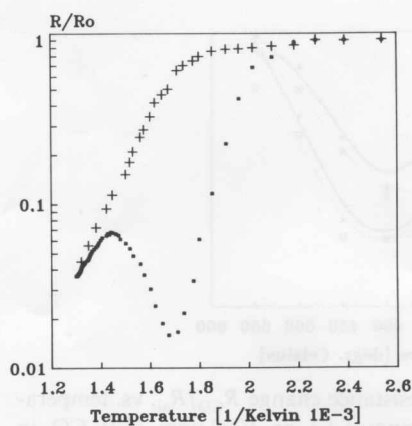
diameters between 0.2 and 1 μm . The orientation of the grains is random, as confirmed by comparison of the X-ray diffraction diagram of SnO_2 powder and SnO_2 thick-film layers (Fig. 3) on Al_2O_3 substrates after firing.

Figure 4(a) gives a typical result for the first run on the relative change in resistance R/R_0 as a function of temperature under synthetic air. R_0 is the sensor resistance at room temperature measured in the externally heated test chamber with a heating rate of 3.5 K/min and a cooling rate of 1.5 K/min.

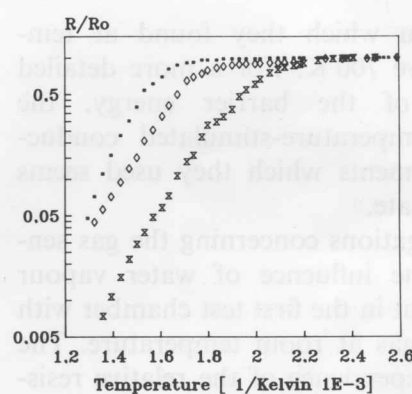
The strong resistance difference between the heating and the cooling run becomes smaller and eventually vanishes after three or four cycles of heating and cooling if the sensor is kept in the second test chamber.

These measurements were performed on sensors with conduction pad distances of 40, 200 and 400 μm and SnO_2 layers covering all conduction leads or printed only between the conduction leads. Figure 4(b) shows the cooling run for three sensor geometries. Except for the slightly different slope and room-temperature resistance R_0 , all sensors behave in the same way. The temperature dependence of the conductance of polycrystalline n-type SnO_2 may be described by [6]

$$G = G_0 \exp(-eV_s/kT)$$



(a)



(b)

Fig. 4. Resistances of thick-film sensors with 200 μm spacing of the electrode structure (a) as a function of inverse temperature for the first heating (\square) and cooling ($+$) runs and with electrode spacings of 40 μm (\times), 200 μm (\diamond) and 400 μm (\square) (b) for the cooling run only.

Here eV_s is the intergranular surface barrier energy and G_0 a factor including the bulk conductance. Assuming that V_s is constant at temperatures between 620 and 710 K, it was determined from the slope of the cooling runs for the three sensor geometries. Barrier energies of 0.9 eV (400 μm), 0.6 eV (200 μm) and 0.68 eV (40 μm) were found. These values are between the barrier heights of TGS sensors (0.5–0.62 eV) and of thick-film sensors (1.2–1.3 eV) reported by Lantto *et al.* [7]. Our assumption of a constant V_s is based on its

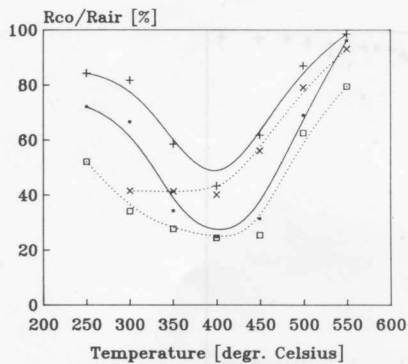


Fig. 5. Relative resistance change R_{CO}/R_{air} vs. temperature due to 250 ppm (+) or 1000 ppm (□) CO in synthetic air. The dotted lines show the influence of a Pt catalyst in each case. The lines are drawn as guides for the eye.

small variation which they found at temperatures above 700 K. For a more detailed investigation of the barrier energy, the method of temperature-stimulated conductance measurements which they used seems more appropriate.

The investigations concerning the gas sensitivity and the influence of water vapour were carried out in the first test chamber with the incoming gas at room temperature. The temperature dependence of the relative resistance change R_{CO}/R_{air} on switching from air to air/CO mixtures is shown in Fig. 5. For an undoped SnO_2 sensor the maximum resistance change of 70% is around 400 °C. Introducing a catalyst increases the resistance change and therefore the gas sensitivity in the temperature range 250 to 400 °C. The relative resistance is also affected by the presence of water vapour. Figure 6 shows the relative resistance change R_{wet}/R_{dry} for temperatures from 200 to 550 °C when air saturated with water vapour (dew point 23 °C) strikes the gas sensor. The resistance drop has a maximum at 300 °C, which becomes less pronounced for sensors with Pd catalyst. This resistance minimum is also found when heating a sensor for the first time (Fig. 4) and may result from the O^- formation and water vapour desorption [8]. At temperatures above 400 °C the resistance decreases linearly, which means less sensitivity to water vapour.

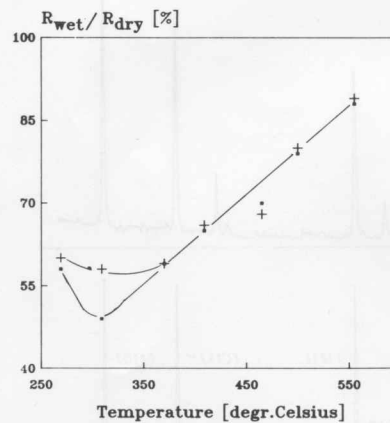


Fig. 6. Relative resistance change R_{wet}/R_{dry} vs. temperature in the range 200 to 550 °C due to wet air (□, without Pd catalyst; +, with Pd catalyst).

An important parameter for the sensor application is the response time. Here we have investigated the time dependence of the resistance change when switching the gas flow through the first test chamber from dry air to air/200 ppm CO and vice versa. The gas change is done in each case after the sensor resistance has stabilized at a constant value. From the time-dependent measurements the time constants t_{on} and t_{off} are determined and plotted against the inverse temperature on Fig. 7. Both time constants decrease exponentially from 200 to 2 s when the temperature increases from 300 to 500 °C. The switch-off time is always longer than the switch-on time and both time constants are lowered by coating the sensor with a Pt catalyst.

For some applications it might be useful to operate the sensor in an a.c. network where the frequency response at constant temperature and gas flow must be known. The results for the complex impedance and the capacitance versus frequency are plotted in Fig. 8. As expected from the resistance decrease with temperature, the impedance decreases in the same way, but this is partially compensated by the increasing capacitance.

Conclusions

Thick-film SnO_2 gas sensors show good CO sensitivity and a sufficiently short response

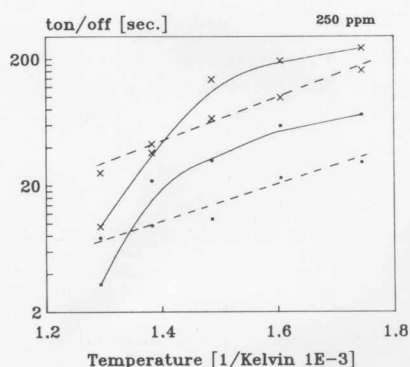


Fig. 7. Time constants t_{on} and t_{off} vs. the inverse temperature (t_{on} = switching from air to test gas, t_{off} = switching from test gas to air). Lines are only drawn as guides for the eye, with dotted lines indicating presence of Pt catalyst (\square , test gas; \times , synthetic air).

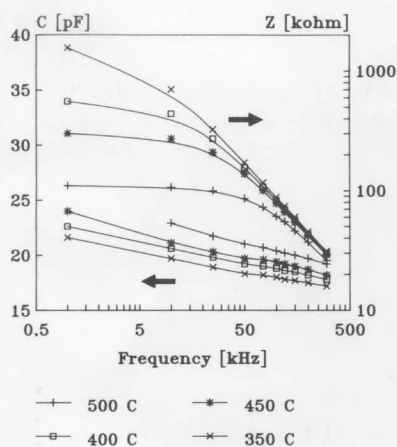


Fig. 8. Frequency dependence of the impedance Z and the capacitance C of the sensor at different temperatures between 350 and 500 °C.

time at operating temperatures of 450 °C, but further investigations concerning the stability and the influence of other gases are required.

Acknowledgements

We wish to thank Leopold Kostal GmbH for supporting this work.

References

- 1 H. P. Hübner and E. Obermeier, Gassensoren auf der Basis von Metalloxid-Halbleitern, *Tech. Mess.*, 52 (1985) 59–66.
- 2 K. Ihokura, Application of sintered tin(IV) oxide for gas detectors, *NTG-Fachtagung VDI/VDE*, Vol. 79, 1982, pp. 312–317.
- 3 Y. Iwata *et al.*, Elektrische Vorrichtung und Verfahren zur Steuerung der Klimaanlage eines Kraftfahrzeuges, *DE-OS 2 941 305* (1980).
- 4 P. Romppainen, H. Torvela, J. Väänänen and S. Leppävuori, Effect of CH_4 , SO_2 and NO on the response of an SnO_2 -based thick-film gas sensor in combustion gases, *Sensors and Actuators*, 8 (1985) 271–279.
- 5 D. Janning, Leitfähigkeitsuntersuchungen an SnO_2 -Schichten auf Dickschichtbasis, *Diploma Thesis*, Soest, F.R.G., 1990.
- 6 S. R. Morrison, Semiconducting gas sensors, *Sensors and Actuators*, 2 (1982) 329–341.
- 7 V. Lantto, P. Romppainen and L. Leppävuori, A study of the temperature dependence of the barrier energy in porous tin dioxide, *Sensors and Actuators*, 14 (1987) 149–163.
- 8 J. F. McAleer, P. T. Mosely, J. O. W. Norris and D. E. Williams, Tin dioxide gas sensors, *J. Chem. Soc., Faraday Trans.*, 83 (1987) 1323–1346.